Potential Energy Function for Cation–Peptide Interactions: An *Ab Initio* Study

BENOÎT ROUX*

Groupe de Recherche en Transport Membranaire, Département de Physique, Université de Montréal, C.P. 6128, succ. A, Canada H3C 3J7

MARTIN KARPLUS

Department of Chemistry, Harvard University, 12 Oxford St., Cambridge, Massachusetts 02138

Received 21 February 1994; accepted 12 September 1994

ABSTRACT

A potential energy function is developed to represent the interaction of small monovalent cations, Li^+, Na^+, and K^+, with the backbone of polypeptides. The results are based on *ab initio* calculations up to the 6-31G* level of the interactions of the ions with acetamide and *N*-methylacetamide. Basis set superposition errors are corrected with the counterpoise method. A systematic overestimate of the bond polarities is taken into account by an empirical scaling procedure that uses the ratio of the experimental to *ab initio* dipole moment. The calculated binding energies obtained with this procedure show consistent convergence with different basis sets and are in good agreement with experimental data on cation–water and cation–dimethylformamide systems. Investigations of the calculated *ab initio* potential energy surface indicate that the cation–peptide interaction is dominated by electrostatics and includes a nonnegligible contribution from polarization of the peptide group by the ion. The induced polarization results in a steeper-than-Coulombic interaction and cannot be described by fixed ion–peptide partial charges electrostatics. Atomic polarizabilities located on the atoms of the ligand molecule are introduced to account for the induced polarization in the empirical energy function. A $\sim 1/r^4$ attractive interaction appears in the potential function. The resulting radial and angular dependence of the potential energy surface is well reproduced.

*Author to whom all correspondence should be addressed.

Journal of Computational Chemistry, Vol. 16, No. 6, 690–704 (1995)

CCC 0192-8651 / 95 / 060690-15

Introduction

Attempts to understand the microscopic factors controlling the passage of ions through narrow transmembrane pores, such as the gramicidin channel, provide a difficult challenge to theoretical approaches based on detailed atomic models.[1-11] The permeation process through the gramicidin channel involves the partial dehydration of an ion,[12] followed by the translocation through the interior of a narrow pore.[13] The ion–channel interactions are dominated by the carbonyl oxygen of the peptide backbone (see Fig. 1).[4,8] An ion such as Na^+ in local minima interacts strongly with four carbonyls and two waters. Thus, the effective potential in the channel and the stabilization relative to aqueous solution depend on an accurate representation of the different interactions. The large hydration energy of ions, around -100 kcal/mol for Na^+,[14] contrasts with the activation energies deduced experimentally for ion transport across the gramicidin channel, which often do not exceed a few k_BT.[15] Although molecular dynamics techniques are being used to study biological systems of increasing complexity,[16] theoretical investigations of processes involving the association of small metal ions to specific protein sites are particularly difficult because ion–peptide association results from a delicate balance of strong interactions. For meaningful theoretical studies of ion–protein association, in general, and of ion transport, in particular, it is necessary to have an accurate and realistic potential function representing the microscopic interactions.

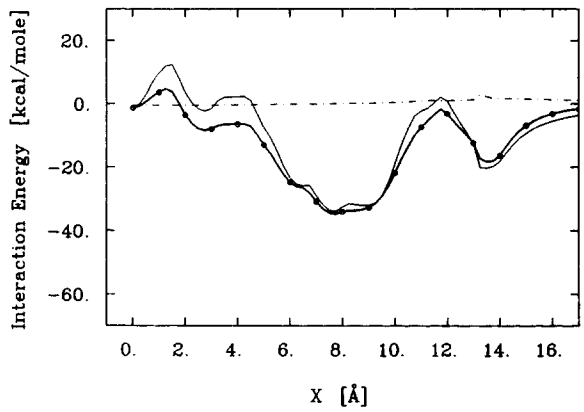

FIGURE 1. Interaction energy profile of a +1 charge Lennard-Jones sphere along the *X*-axis of the gramicidin A channel. The total interaction (bold line with circles), the electrostatic interaction between the C=O and the ion (solid line), and the interaction with the sidechains (dash-dotted line) are shown. The center and the entrance of the channel are located at 0 and 13 Å, respectively. For each *X*, the position of the ion was optimized in the cross section of the channel; no truncation was applied to the nonbonded interactions; the value of the dielectric constant was set to one. The structure of the gramicidin, the right-handed head-to-head dimer determined experimentally from 2D NMR in detergent micelles,[13] is maintained rigidly for all the calculations. The Lennard-Jones parameters of the ion, chosen to approximate a Na^+, are from Mackay et al.[1]

Gas phase experiments and *ab initio* studies of model systems provide the most direct information concerning the individual microscopic interactions. For example, gas phase ion–cluster equilibria experiments have been used to measure the binding energy of the alkali ions to one or more water molecules.[17,18] Unfortunately, due to the instability of peptides at high temperature,[19] the measurements of ion–peptide interactions are scarce. The binding energies of K^+ to dimethylacetamide and to dimethylformamide (DMF) have been measured using mass spectroscopy;[20] there are also estimates of Li^+ affinity for DMF[21] and for formaldehyde[22] from cyclotron resonance spectroscopy. The data indicate that the interactions of cations with model peptides are substantially larger than with water (e.g., the binding enthalpy of K^+ with a water molecule is 17 kcal/mol and 31 kcal/mol with a molecule of DMF). *Ab initio* calculations performed on small model systems supplement the information available from experiments. Detailed *ab initio* studies have been reported on the interaction of ions with model peptide molecules such as formaldehyde, acetamide, formamide, DMF and *N*-methylacetamide (NMA).[23-32] Most calculations in the literature were done with semiempirical or relatively low-level *ab initio* methods and restricted basis sets. Semiempirical methods have been used to study Li^+ binding to carbonyls[23] and sodium to NMA;[24] *ab initio* methods at the Hartree-Fock level have been used to study the affinity of lithium[25] and potassium for Lewis bases,[26] charge reorganization in NMA–sodium complexes,[27] cation interactions with alkyl-substituted amides,[28,31,32] and lithium, sodium, and potassium interactions with formaldehyde.[29] Although the calculations provide interesting information on the nature of the interaction, quantitative knowledge of the interactions between alkali ions and peptide units is incomplete.

The goals of the present study are to assess the cation–peptide interaction and develop an accurate and computationally simple potential energy function to be used in molecular dynamics simulations. Due to the lack of direct experimental data on ion–peptide interactions, the approach is based primarily on high-level *ab initio* calculations of cation interactions with small model systems containing the peptide group. It is found that the cation–peptide interactions include an important contribution from polarization induced by the ion. A simple analytical potential function describing the ion–peptide interactions is constructed and parameterized to fit the results from *ab initio* calculations. The polarization effects are included in the potential energy function by introducing an ion-induced dipole interaction ($\sim -1/r^4$) whose magnitude is determined by the atomic polarizabilities located on the atoms of the ligand molecule. Except for this important addition, the potential function for the interactions is identical in form to many others used in molecular dynamics of biological macromolecules[16,33-37] (i.e., it is based on a sum of radially symmetric pair decomposable site–site functions including Coulomb partial charges electrostatics, core repulsion, and van der Waals dispersion). The ion–peptide potential energy function is consistent with the protein energy function used in the CHARMM program.[38] The combined energy function has been used to calculate the potential of mean force and the rate of transport of Na^+ and K^+ in the gramicidin channel.[8-10] Future work and possible improvements of the parameterization are discussed.

Method and Computational Details

AB INITIO CALCULATIONS

The acetamide and NMA molecules were chosen to model the carbonyl group of the peptide backbone. Preliminary *ab initio* calculations showed that formaldehyde has weaker electrostatic interactions and does not provide a satisfactory model for ion-backbone interactions. This is supported by the large difference between the experimental binding enthalpy of Li^+ to formaldehyde and DMF; the values are 38 and 48 kcal/mol for lithium with formaldehyde and DMF, respectively.[17,18,20,21] The acetamide and NMA molecules give a realistic representation of the electronic structure of the backbone by conserving the first (C) and second (N, CH_3) neighbors of the oxygen. A substitution of the N—H by a N—CH_3 in the NMA molecule allows a more complete investigation of the electrostatic and steric influence of the C_α in a peptide backbone. Calculations of the binding enthalpy of cations with water and DMF, for which experimental data are available,[17,18,21,20] are used to test the accuracy of the potential energy surface of cations with acetamide and NMA.

The *ab initio* interaction energies of water, DMF, acetamide, and NMA with Li^+, Na^+, and K^+ were calculated using the Gaussian 82[39] and Gaussian 86[40] programs with the 3-21G, 3-21G*, 6-31G, and the 6-31G* basis sets.[41-46] A contraction of the basis set of Wachters[47] by Clementi[48] was used for the K^+ ion calculations at the 6-31G level. The 3-21G and 6-31G basis set coefficients for K^+ are given in Appendix A. The 6-31G* basis set was chosen because it generally yields satisfactory results for proton, lithium, and sodium affinities.[49] Calculations using the less extended basis sets were performed to provide a comparison and give some indication of the convergence.

In the calculations, the experimental internal gas phase geometry of the water,[50] the acetamide,[51] and the NMA[52] molecules were maintained. For DMF, the geometry optimized at the 4-31G level was used[53] (but see ref. 54). The potential energy surface of Li^+ and Na^+ with acetamide was explored along three directions (r, θ, ϕ) around the carbonyl oxygen of the acetamide molecule (see Fig. 2): that is, as a function of the oxygen–ion distance along the C=O axis (r), as a function of the C=O–ion angle out (θ), and in (ϕ) the H—N—C=O plane at a fixed oxygen–ion distance (3 Å). The value of r = 3 Å was chosen for the angular exploration around the carbonyl oxygen because this provides information about the variation of the potential energy near the dominant energy well.

Systematic errors in the results obtained from Hartree-Fock (HF) *ab initio* calculations with split valence basis sets (i.e., basis superposition error and overestimated dipole moments) must be addressed to extract useful semiquantitative information. The basis set superposition correction was estimated by removing the interaction with a ghost ion particle using the "functional counterpoise method";[55] counterpoise corrections with a ghost ligand (water, acetamide, DMF, and NMA) were not considered. In the optimized geometry, the basis set superposition correction was in the range of 1 to 2 kcal/mol for the 6-31G and 6-31G* calculations, and 8 to 10 kcal/mol for the 3-21G and 3-21G* calculations. The dominant contribu-

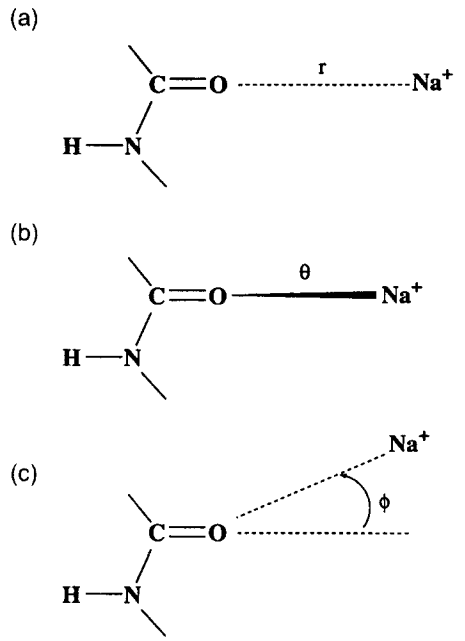

FIGURE 2. The potential energy surface was explored as a function of (a) the oxygen–ion distance r along the C=O axis, (b) the C=O–ion angle θ out of the H—N—C=O plane, and (c) the C=O–ion angle ϕ in the H—N—C=O plane. For θ and ϕ, the ion–oxygen distance was fixed at 3 Å.

tion to the ion–molecule interactions are charge transfer, ion-molecular dipole electrostatic interaction, and ion-induced polarization energy.[56] Because the dipole moments of polar molecules calculated with split valence basis sets are known to be too large due to overestimated bond polarities,[57–59] the calculated affinities are expected to be too large. To account for the systematic errors due to basis set superposition and overestimated dipole moments, all the interactions energies were corrected according to the equation

$$E_{\text{correc}}(\mathbf{r}_i) = \frac{\mu_{\text{exp}}}{\mu_{\text{scf}}}(E_{\text{scf}} - E_{\text{bsse}}) \qquad (1)$$

where μ_{exp} and μ_{scf} are the experimental and the computed *ab initio* electric dipole of the molecule in the absence of the ion and E_{bsse} is the correction for the basis set superposition error. The experimental[60,61] to *ab initio* dipole ratios given in Table I are on the order of 0.8 to 0.9. All the self-consistent field (SCF) potential energies were corrected according to eq. (1). Further tests showed that the present results did not vary significantly when the calculations were performed using Møller-Plesset second-order perturbation theory (data not shown), indicating that electron correlation is not essential for the present investigation of ion–molecule interactions. Zero point vibration energy corrections, which must be included to compare the calculated and experimental values, were estimated from the vibrational frequencies calculated at the HF/6-31G** level for the cation–water complexes (see Appendix B); they are on the order of 0.75 kcal/mol.[62]

TABLE I.
Dipole Scaling Factors.

Molecule	Reference	Dipole (D)	Scaling
Water	Experimental[a]	1.855	1.00
	HF/3-21G	2.43	0.76
	HF/3-21G*	2.43	0.76
	HF/6-31G	2.63	0.70
	HF/6-31G*	2.23	0.82
	HF/6-31G**	2.18	0.85
	TIP3P[c]	2.35	0.79
Dimethyl-formamide (DMF)	Experimental[b]	3.81	1.00
	HF/3-21G	4.175	0.91
	HF/3-21G*	4.175	0.91
	HF/6-31G	4.635	0.82
	HF/6-31G*	4.292	0.89
Acetamide	Experimental[a]	3.73	1.00
	HF/3-21G	4.039	0.92
	HF/3-21G*	4.039	0.92
	HF/6-31G	4.405	0.86
	HF/6-31G*	4.123	0.90
	Potential function[c]	4.07	0.92
N-methyl-acetamide (NMA)	Experimental[b]	3.76	1.00
	HF/3-21G	3.885	0.97
	HF/3-21G*	3.885	0.97
	HF/6-31G	4.247	0.89
	HF/6-31G*	4.192	0.94
	Potential function[c]	4.191	0.90

[a]From ref. 60.
[b]From ref. 61.
[c]The scaling for the empirical potential energy function is the ratio of the dipole moment calculated from the partial charges in Table VI and the experimental values.

POTENTIAL ENERGY FUNCTION

The ion-peptide interactions are represented by a sum of pairwise additive interactions of the form

$$E = \sum_j E_{\text{elec}}(r_{ij}) + E_{\text{core}}(r_{ij}) + E_{\text{vdW}}(r_{ij}) + E_{\text{pol}}(r_{ij}) \qquad (2)$$

where the various terms are

$$E_{\text{elec}}(r_{ij}) = \frac{q_i q_j}{|\mathbf{r}_i - \mathbf{r}_j|}$$

$$E_{\text{core}}(r_{ij}) = \frac{A_{ij}^{(n)}}{|\mathbf{r}_i - \mathbf{r}_j|^n}$$

$$E_{\text{vdW}}(r_{ij}) = -\frac{B_{ij}^{(6)}}{|\mathbf{r}_i - \mathbf{r}_j|^6}$$

$$E_{\text{pol}}(r_{ij}) = -\frac{\alpha_j q_i^2}{2|\mathbf{r}_i - \mathbf{r}_j|^4} \qquad (3)$$

where q_i and $\mathbf{r}_i$ are the charge and the position of the ion and q_j, $\mathbf{r}_j$, and α_j are the partial charge, the position, and the polarizability of the jth peptide atom.

The standard combination rule[38] is used to generate the Lennard-Jones 6–12 coefficients [i.e., $A_{ij}^{(12)} = 4\epsilon_{ij}\sigma_{ij}^{12}$ and $B_{ij}^{(6)} = 4\epsilon_{ij}\sigma_{ij}^{6}$, with $\sigma_{ij} = (\sigma_i + \sigma_j)/2$ and $\epsilon_{ij} = \sqrt{\epsilon_i \epsilon_j}$]. All the core energy terms were represented by a $1/r^{12}$ repulsion ($n = 12$) except the ion–carbonyl oxygen, which is represented by a $1/r^8$ repulsion ($n = 8$). In describing the interaction with acetamide or NMA, only the first-order polarization induced by the ion is included (i.e., the partial charges of the peptide as well as other induced dipoles do not influence a particular induced dipole and the polarization is not calculated self-consistently). The importance of higher order contributions to the polarization energy in larger systems is examined elsewhere.[63]

The partial charges and the Lennard-Jones parameters assigned to the peptide backbone were taken from previous work on peptide–peptide potential.[38,58] The adjustment of the remaining parameters, aimed at reproducing the salient features of the *ab initio* potential energy surface, involved an interative procedure that was carried out manually. Automatized least-squares fitting procedures, such as used in other studies,[31,32] did not produce satisfactory results because the problem is not sufficiently overdetermined. The polarizability coefficients, α_i, were adjusted iteratively from the radial and angular dependence of the potential energy surface of Li^+ and Na^+ with acetamide. The procedure exploited the fact that the variation of the potential energy surface along the three directions r, θ, and ϕ does not depend on the atomic polarizability of the atoms that remain at a constant distance from the ion because the total ion-induced polarization E_{pol} is represented by a sum of pairwise additive terms in eqs. (2) and (3). Thus, the variations of the potential function along r, θ, and ϕ are dominated by the polarizability assigned to the oxygen (O), to the carbonyl carbon (C), and to the nitrogen (N) and methyl group (CH_3), respectively. In a first step, the oxygen polarizability was adjusted based on the potential surface in the interval from 2 to 5 Å along the ion–carbonyl oxygen distance (r); in a second step, the carbonyl carbon polarizability was adjusted based on potential surface along the C=O–ion angle out of the H—N—C=O plane (θ); and in a third step, the methyl group and nitrogen polarizabilities were adjusted based on the potential surface along the C=O–ion angle in the H—N—C=O plane (ϕ). The oxygen atom was chosen as the reference center for the angular exploration because the ion–oxygen pair interaction makes the largest contribution to the total ion–acetamide interaction energy in the potential function based on eqs. (2) and (3). The procedure was repeated until a satisfactory fit was obtained simultaneously for Li^+ and Na^+ and the results were extended to K^+. Finally, the cation–oxygen core parameters, $A^{(8)}$ and $B^{(6)}$, were adjusted to reproduce the energy and geometry of the optimized complex of Li^+, Na^+, and K^+ with acetamide. All the final parameters are listed in Table VI.

Results and Discussion

The results on the cation–water systems are given in Table II, and in Figure 3. Table II lists the *ab initio* and experimental energies for ion–water complexes. Figure 3 shows the Na^+–water interaction energy as a function of distance along the water dipole axis in the oxygen direction. The calculated interaction before and after the correction based on eq. (1) are shown. The *ab initio* interaction energies of the cations with DMF, acetamide, and NMA are given in Tables III, IV, and V. The potential energy surfaces of Na^+ with acetamide, before and after the correction, are shown in Figure 4 The surfaces for Na^+ and Li^+ after correction are shown in Figures 5 to 10†; all surfaces were corrected according to eq. (1). The results obtained with the potential energy function are included in Tables I, IV, and V.

The angular dependence of the potential is almost identical for Li^+ (Figs. 9 and 10) and Na^+

†Figures 9 to 12 are available from the authors upon request as supplementary material.

TABLE II.
Optimized Geometry with Water and Corresponding Interaction Energies.

Ion	Model	Distance (Å)	Energy (kcal / mol) SCF	Corrected
Li^+	HF / 3-21G	1.77	48.14	36.7
	HF / 6-31G	1.82	46.78	32.0
	HF / 6-31G*	1.86	39.63	32.0
	HF / 6-31G**	1.85	39.73	33.8
	Experimental[a]	—	—	34.0
Na^+	HF / 3-21G	2.12	41.15	24.7
	HF / 3-21G*	2.11	43.34	25.8
	HF / 6-31G	2.17	33.93	24.0
	HF / 6-31G*	2.21	28.69	24.0
	HF / 6-31G**	2.21	28.68	24.0
	Experimental[a]	—	—	24.0
K^+	HF / 3-21G	2.58	27.30	15.9
	HF / 3-21G*	2.55	32.13	17.6
	HF / 6-31G	2.60	23.04	15.8
	Experimental[a]	—	—	16.9

[a]From ref. 18.

TABLE III.
Optimized Geometry with Dimethylformamide and Corresponding Interaction Energies.

Ion	Model	Distance (Å)	Energy (kcal / mol) SCF	Corrected
Li^+	HF / 3-21G	1.68	71.74	58.5
	HF / 6-31G	1.72	63.86	51.0
	HF / 6-31G*	1.75	58.02	49.7
	Experimental[a]	—	—	48
Na^+	HF / 3-21G	2.03	52.08	40.9
	HF / 3-21G*	2.02	55.71	43.3
	HF / 6-31G	2.07	46.72	37.1
	HF / 6-31G*	2.11	42.72	36.4
	Experimental	—	—	—
K^+	HF / 3-21G	2.47	35.08	27.1
	HF / 3-21G*	2.43	41.42	30.3
	HF / 6-31G	2.48	32.51	28.4
	Experimental[b]	—	—	31

[a]Lower limit estimate from ref. 21.
[b]From ref. 20.

(Figs. 6 and 7) at a distance of 3 Å away from the oxygen. For both Li^+ and Na^+, the potential energy increases smoothly from −23 to −12 kcal/mol as the ions are moved in the direction perpendicular to the amide plane to an angle θ equal to 90°. There is a broad well as the ions are displaced in the amide plane. The substitution of one hydrogen bonded to the nitrogen in acetamide by a methyl group in NMA has a significant influence on the ϕ-dependence due to the repulsive ion–methyl steric interaction. Small differences are observed between the potential surface of the two ions with ϕ around 60–70 degrees in Figures 11 and 12 due to the difference in ion size. Nevertheless, the results indicates that the cation–acetamide potential surface is dominated by electrostatic in-

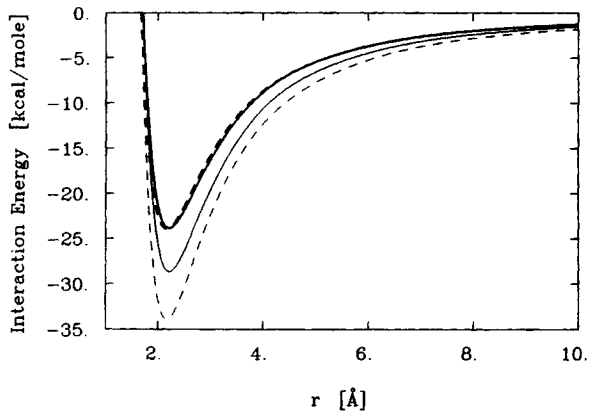

FIGURE 3. Water–Na^+ *ab initio* interaction energy as a function of the oxygen ion distance *r* (the hydrogens pointing away from the ion). The interaction energy is overestimated in the uncorrected *ab initio* HF / 6-31G (thin dashed line) and HF / 6-31G* (thin solid line). The HF / 6-31G* and HF / 6-31G agree well at all distances after correction (bold lines). The HF / 6-31G** energy surface is virtually identical to that of the HF / 6-31G* and is not shown for the sake of clarity.

TABLE IV.
Optimized Geometry with Acetamide and Corresponding Interaction Energies.

Ion	Model	Distance (Å)	Energy (kcal / mol) SCF	Corrected
Li^+	HF / 3-21G	1.68	70.65	57.9
	HF / 6-31G	1.72	61.80	51.0
	HF / 6-31G*	1.75	56.41	49.1
	Potential function	1.82	—	51.0
Na^+	HF / 3-21G	2.03	51.47	40.4
	HF / 3-21G*	2.02	55.11	43.1
	HF / 6-31G	2.07	43.51	36.9
	HF / 6-31G*	2.10	39.82	36.0
	Potential function	2.10	—	36.3
K^+	HF / 3-21G	2.47	34.87	26.7
	HF / 3-21G*	2.44	41.30	29.9
	HF / 6-31G	2.49	31.49	26.2
	Potential function	2.50	—	29.2

TABLE V.
Optimized Geometry with NMA and Corresponding Interaction Energies.

Ion	Model	Distance (Å)	Energy (kcal/mol) SCF	Energy (kcal/mol) Corrected
Li^+	HF/3-21G	1.71	68.15	58.3
	HF/6-31G	1.72	63.14	54.1
	HF/6-31G*	1.74	57.57	52.6
	Potential function	1.81	—	51.6
	Lennard-Jones 6–12	1.80	—	41.1
Na^+	HF/3-21G	2.06	49.13	40.4
	HF/3-21G*	2.04	52.60	42.6
	HF/6-31G	2.07	46.17	39.3
	HF/6-31G*	2.10	42.36	38.4
	Potential function	2.10	—	38.1
	Lennard-Jones 6–12	2.10	—	32.5
K^+	HF/3-21G	2.47	35.29	28.4
	HF/3-21G*	2.43	41.79	31.7
	HF/6-31G	2.53	28.48	24.8
	Potential function	2.49	—	30.7
	Lennard-Jones 6–12	2.50	—	25.2

teractions even at a relatively short ion–oxygen distance (r = 3 Å).

The correction based on eq. (1) should be strictly valid at large cation–ligand distances, when the energy is dominated by the interaction of the ion with the constant dipole of the ligand. Assuming that the charge–dipole interaction is dominating at all distances, the correction with eq. (1) is extended to the whole potential energy surface. Prior to the correction based on eq. (1), the 6-31G and 6-31G* potential energy surfaces shown in Figure 3 differ significantly; the *ab initio* energies differ by 4 to 7 kcal/mol in the case of Li^+ and Na^+ ions and disagree with the experimental values (see Table

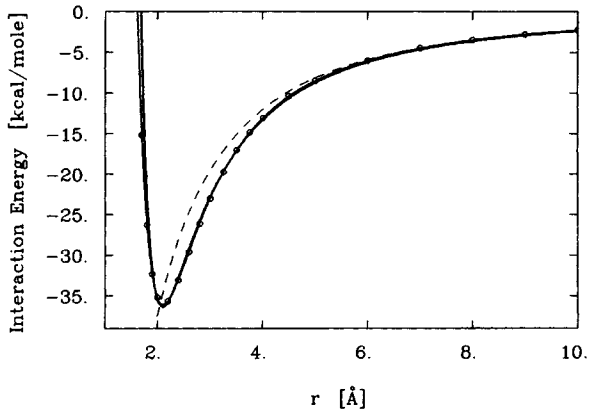

FIGURE 5. Acetamide–Na^+ interaction energy as a function of the oxygen ion distance r (the ion is moving along the C=O bond). The modified CHARMM empirical energy function (bold line) and the *ab initio* HF/6-31G* (solid with circles) are shown. The electrostatics contribution from the point charges of acetamide (dashed line), in the absence of the induced polarization, is not sufficient to model the steeper-than-Coulombic interaction in the region from 2.0 to 5.0 Å and underestimates the minimum energy by almost 5 kcal/mol at r = 2.1 Å.

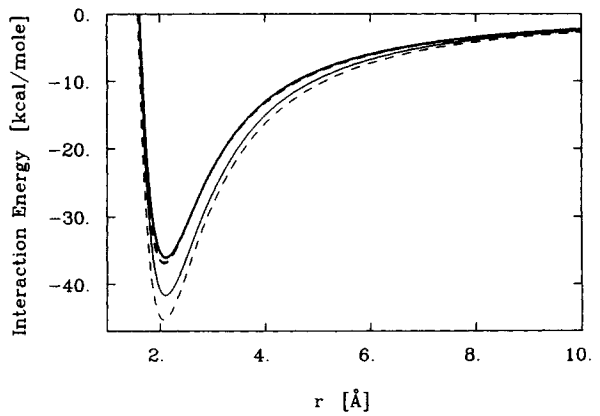

FIGURE 4. Acetamide–Na^+ *ab initio* interaction energy as a function of the oxygen ion distance r (the ion is moving along the C=O bond). The interaction energy is overestimated in the two uncorrected *ab initio* calculations HF/6-31G (thin dashed line) and HF/6-31G* (thin solid line). The HF/6-31G* and HF/6-31G agree at all distances after correction (bold lines).

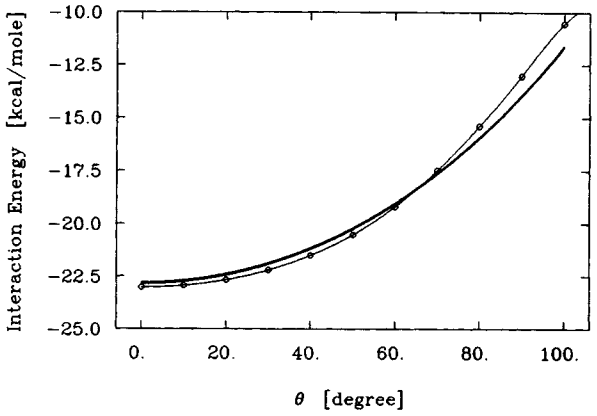

FIGURE 6. Acetamide–Na^+ interaction energy as a function of the C=O–Na^+ angle θ (the ion is moving at a fixed distance of 3.0 Å from the carbonyl oxygen perpendicular to the plane of the H—N—C=O atoms). The modified CHARMM empirical energy function (bold line) and the corrected *ab initio* HF/6-31G* (line with circles) are shown.

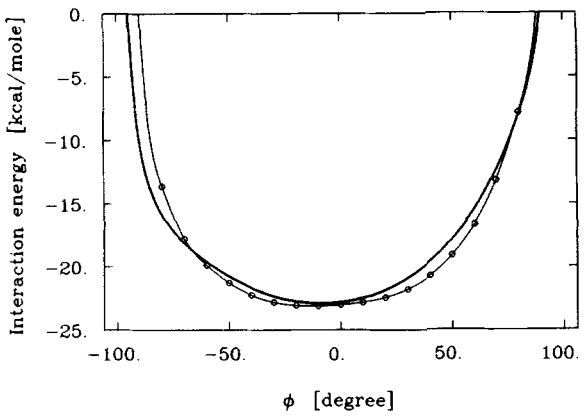

FIGURE 7. Acetamide–Na^+ interaction energy as a function of the C=O–Na^+ angle ϕ (the ion is moving at a fixed distance of 3.0 Å from the carbonyl oxygen in the plane of the H—N—C=O atoms). The modified CHARMM empirical energy function (bold line) and the corrected *ab initio* HF/6-31G* (line with circles) are shown.

II). However, an important feature of the potential energy surface, such as the position of the energy minimum, does not depend strongly on the level of calculation. For example, the cation–oxygen distance in the optimized geometry of all complexes is nearly identical (see Tables II, III, IV, and V). The 6-31G and 6-31G* surfaces are similar at all distances after the energies are corrected with eq. (1). A striking example is provided by the Li^+–water interaction at the 6-31G level. It is reduced by the correction from 46.78 to 32.0 kcal/mol, which is only 2 kcal/mol less than the

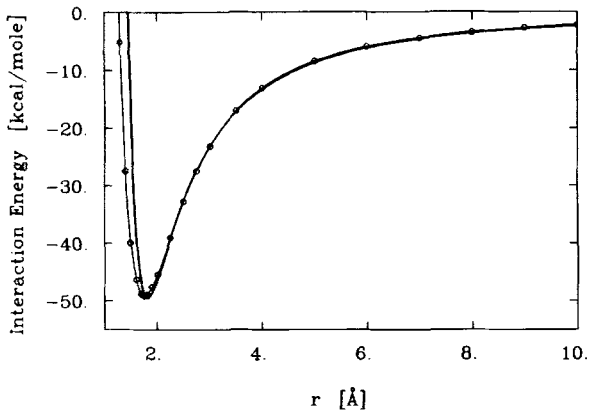

FIGURE 8. Acetamide–Li^+ interaction energy as a function of the oxygen ion distance r (the ion is moving along the C=O bond). The modified CHARMM empirical energy function (bold line) and the corrected *ab initio* HF/6-31G* (line with circles) are shown.

experimental value. Moreover, application of the corresponding correction to the higher level (6-31G**) calculation yields almost exact agreement with experiments, as shown in Table II. Similar results are obtained for other ions. The calculated cation–water binding energies are in accord with previous *ab initio* studies of cation–water systems.[49,64]

The Li^+ and Na^+ *ab initio* interaction energies with acetamide are found to converge to a unique value with the different basis sets (see Fig. 4) and agree well with experimental data.[17] Comparison with the limited experimental gas phase data for DMF indicates that the calculated binding energies have the correct order of magnitude (i.e., the binding energies of Li^+ and K^+ with DMF are approximately 50 kcal/mol and 30 kcal/mol, respectively). The interactions calculated with the 3-21G basis set are generally in poorer agreement with the experiments. The calculated binding energies involving K^+ are more scattered and do not agree as well with the experimental values. The best agreement with experimental data is obtained with the 3-21G*, although this may be due to a fortuitous cancellation of errors.

The dominant effect of the charge–dipole interaction in the ion–molecule association is also reflected in the optimized geometries of the complexes with model peptides; in the case of water, the optimized position of the ion is directly aligned with the dipole axis by symmetry. The dipole moment of NMA is directed along the C=O bond, pointing from the oxygen to the carbon and tilted by an angle of approximately 10° in the direction of the N. In the complexes with NMA, the optimum positions of Li^+, Na^+, and K^+ are directed along the C=O bond with angles of 8, 7, and 4 degrees away from the N (see Fig. 14). The resulting angle between the cation-to-oxygen vector and the dipole moment of NMA is less than 3°. Thus, the direction of the deviations of the ion position from a linear configuration with the C=O bond are consistent with the dipole moment of the isolated molecule. Moreover, the small deviation from linearity provides only a small gain in binding energy; the difference between the linear and nonlinear configurations is less than 0.06 kcal/mol for all complexes. These observations demonstrate that the cation–peptide binding is dominated by overall electrostatics interactions and not by the geometry of the lone pairs of the carbonyl oxygen.

The ion-induced polarization results in a significant intramolecular electronic charge reorganization.[27] This aspect is illustrated by the Mulliken

populations of acetamide complex with the medium size Na^+ ion shown in Figure 13. In the presence of the ion, the bond polarization tends to be combined with increased charge alternation (e.g., the carbonyl oxygen charge is more negative, the carbonyl carbon charge is more positive, the methyl carbon is more negative, and the methyl hydrogens are more positive). One exception is nitrogen, which is less negative in the presence of the ion. Similar effects have been observed with other calculations at the 4-31G level.[27] The effects as expressed by Mulliken populations are somewhat reduced when the 6-31G* rather than the 6-31G basis set is used. This is due presumably to the more effective local polarization (without atomic population changes) in the latter. Little charge transfer from the ion to the acetamide takes place, however. There is a charge transfer of approximately -0.08 to -0.10 e from the acetamide molecule to the Na^+. The charge transfer may be partly due to a basis set superposition error because the presence of the ion orbitals contributes to delocalize the partial charge away from the carbonyl oxygen. These results suggest that it is reasonable to neglect ion–ligand charge transfer in the present cation-model peptide systems but that the ion-induced polarization must be accounted for in the potential energy function. An interaction term characteristic of ion-induced polarization is required to reproduce the distance dependence of

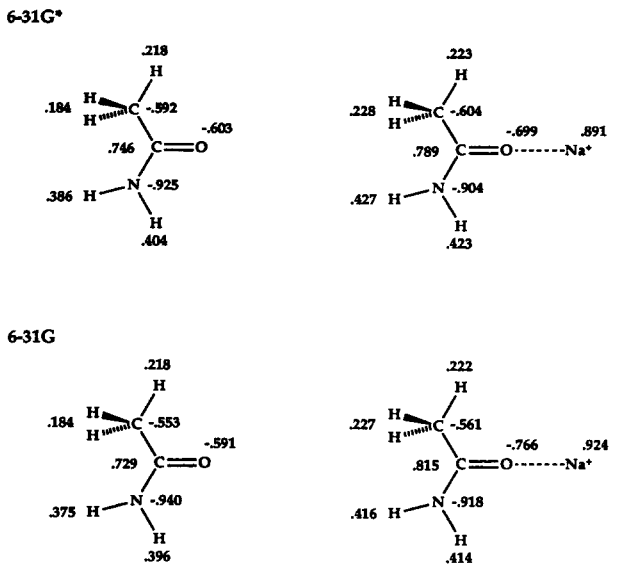

FIGURE 13. Acetamide–Na^+ Mulliken population analysis for the HF / 6-31G(*) basis sets (a) in the absence of Na^+ and (b) in the presence of Na^+ at the optimized oxygen–ion distance.

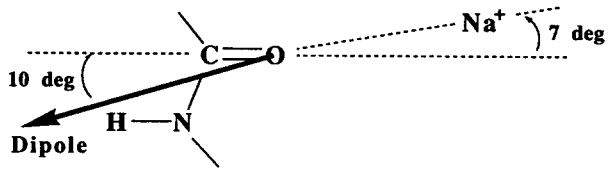

FIGURE 14. Schematic representation of the orientation of the dipole moment of NMA relative to the optimized position of sodium.

the ion–peptide interaction in the range of 2 to 5 Å (see Figs. 5 and 8). As shown in Figure 5, the steeper-than-Coulombic distance dependence of the ion–peptide interaction cannot be obtained with the electrostatic interactions of fixed partial charges, such as used in most biomolecular potential energy functions.[16] The importance of ion-induced polarization in ion–peptide interactions was recognized by Clementi and Conrogiu, although it was not included explicitly in their potential energy function.[31,32] Polarization effects appear to be less important in the case of ionic aqueous solutions,[65] and standard nonpolarizable models have been extensively parameterized to yield accurate results.[66]

As noted by several authors,[25,32] the affinity of small metal cations for the oxygen of the —N—C=O functional group is much larger than the corresponding cation–water interactions. The binding energies are 52.6, 38.4, and 27 kcal/mol for Li^+, Na^+, and K^+ with NMA; this is approximately 1.5 times the cation–water interaction (see Tables II and V). In part, the large interaction can be understood in terms of the properties of the isolated ligand molecules. A first contribution arises from the larger permanent dipole of the amide group relative to that of water [i.e., in the gas phase, the dipole moment of the NMA molecule is 3.76 Debye, which is twice as large as the water dipole (1.855 Debye)]. A second contribution to the interaction energy arises from the larger polarizability of the amide group. The experimental value of the polarizability of NMA is 7.82 $Å^3$, whereas that of water is 1.45 $Å^3$.[67] Although a direct correspondence between the experimental value of the dipole moment and total polarizability of the amide molecules in the gas phase and those based on the partial charges and the atomic polarizability coefficients in the potential function is not expected, they have a similar magnitude; the dipole moment and the total polarizability are 4.19 Debye and 4.3 $Å^3$, respectively,

TABLE VI.
Interaction Parameters[a].

Atom	σ (Å)	ϵ (kcal / mol)	q (e)	α (kcal / mol Å^4 / e)	$A^{(8)}$ (kcal / mol / Å^8)	$B^{(6)}$ (kcal / mol / Å^6)
Li^+	2.3698 (1.6470)	0.0840	1.00		2750	150
Na^+	2.7297 (2.2780)	0.1000	1.00		6200	290
K^+	3.3605 (2.8680)	0.3600	1.00		30,000	3600
C	3.2072	0.0498	0.55	0.3		
O	2.8509	0.1591	−0.55	1.5		
N	2.8509	0.2384	−0.35	1.5		
H	1.4254	0.8000	0.25	0.0		
C_α	3.8576	0.1142	0.10	0.5		

[a]In acetamide the partial charges of N and H are −0.6 and 0.3; in NMA the partial charges of N, H, and CH_3 are −0.45, 0.30, and 0.15 e, respectively. The $A^{(8)}$ and $B^{(6)}$ coefficients apply exclusively to the ion–carbonyl oxygen pair; numbers in parentheses are the alternative cation σ parameters for the specific cation–carbonyl oxygen interactions (see in the text).

for the NMA molecule based on the parameters of Table VI.

The strong interaction with the amide group results in a cation–oxygen distance that is shorter than that in the cation–water complexes. For example, the cation–oxygen distances of Li^+, Na^+, and K^+ with water are 1.85, 2.21, and 2.60 Å, respectively, almost exactly 0.1 Å larger than with the model peptide complexes, where the distances are 1.75, 2.10, and 2.50 Å for Li^+, Na^+, and K^+, respectively. There is a clear relationship between the cation–oxygen distances in the *ab initio* optimized geometries and the standard Pauling ionic radii of Li^+, Na^+, and K^+. The Pauling ionic radii are 0.60, 0.95, and 1.33 Å.[68] This observation may be useful in extending the present parameterization to larger cations, such as Rb^+ and Cs^+, which are difficult to treat accurately by standard *ab initio* methods.

Although the resulting set of parameters is probably not unique, the potential energy surfaces in Figures 5 to 10 agree rather well with the *ab initio* calculations. A function varying as $1/r^8$ was found to reproduce better the cation–carbonyl oxygen core repulsion than the more standard $1/r^{12}$ of the Lennard-Jones 6–12 potential. It has been suggested that softer repulsive functions give a better representation of the core interaction caused by the Pauli exclusion principle for the temperatures normally used in biopolymer simulations.[34,69] However, in most cases the difference in behavior is small (A. MacKerrell and M. Karplus, unpublished calculations). For strong ion-carbonyl oxygen interaction, the use of a softer core was found to be necessary to reproduce the *ab initio* calculations. The other van der Waals interactions were represented by the standard Lennard-Jones 6–12 potential. The van der Waals attractive (dispersion) interaction, varying as $1/r^6$, is included in the empirical energy function even though it is not present in the SCF calculations.

If quantitative accuracy for the magnitude of the interaction energy is not required, it may be useful to have ion–peptide parameters with no ion-induced polarization and the standard Lennard-Jones 6–12 potential. Such a simple energy function may be employed for structural rather than energetic studies (e.g., in crystallographic refinement by simulated annealing with restrained molecular dynamics[70]). A second parameter set without polarization and with the Lennard-Jones 6–12 energy function is given in Table VI. The Lennard-Jones parameters were adjusted to give accurate values for the position of the energy minimum of the cations along the C=O axis with the same value for the van der Waals well depth ϵ as in the more accurate function. The energies and optimized geometry for the cations interacting with NMA using the Lennard-Jones 6–12 model are given in Table V. It is found that the cation–peptide interaction energy is underestimated by about 10, 6, and 4 kcal/mol for Li^+, Na^+, and K^+ ions, respectively. This tendency is indicative of the increasing ion-induced polarization energy for the smaller cations. One could, of course, adjust the Lennard-Jones 6–12 parameters

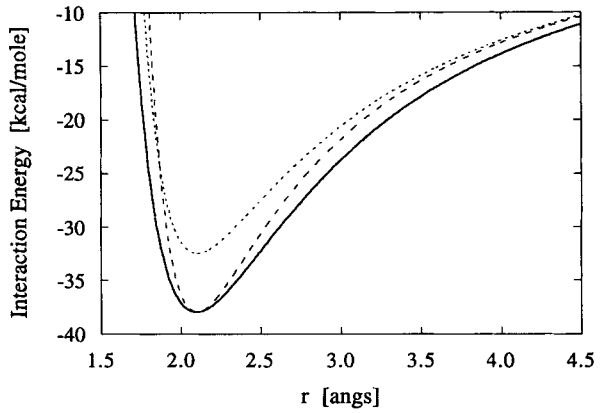

FIGURE 15. Illustration of the importance of constructing the potential function with the essential interactions. The interaction energy of Na^+ with NMA is shown for the empirical potential function, parameterized with ion-induced polarization fitted to the *ab initio* calculations to yield an energy minimum of -38.1 kcal/mol at an oxygen–ion distance of 2.10 Å (solid line). The alternate Lennard-Jones potential function for geometry optimization is parameterized to yield an energy minimum of -32.5 kcal/mol at the same distance with $\sigma = 2.2708$ Å and $\epsilon = 0.1$ kcal/mol according to the standard combination rule (dotted line). The "wrong" Lennard-Jones potential function is parameterized to yield both the position and the depth of the energy minimum with $\sigma = 1.2552$ Å and $\epsilon = 80.96$ kcal/mol according to the standard combination rule (dashed line). In both cases, the Lennard-Jones $1/r^{12}$ repulsion is too steep relative to the potential function with the $1/r^8$ repulsion.

(i.e., the well depth ϵ and the radius σ) to fit both the interaction energy and the position of the minimum. The result of such parameterization is shown in Figure 15. The van der Waals attractive term is too large and the shape of the energy minimum, induced by the attractive $1/r^6$, is unphysically narrow as compared to the better potential energy function. Moreover, the interaction remains underestimated in the region from 3 to 5 Å because the dispersion term, $\sim 1/r^6$, decreases more rapidly than the ion-induced polarization energy, $\sim 1/r^4$. This example illustrates the type of problems that arise when the potential function is constructed without some of the essential interaction energy contributions.

Conclusion

The purpose of this article was to develop an empirical energy function that provides a simple and accurate representation of ion–peptide interactions for Li^+, Na^+, and K^+. Because the experimental data for such systems are limited, the parameterization was based on the results of *ab initio* calculations, which are the only way to obtain detailed information concerning the shape of the potential function. An empirical correction procedure was used to remove the basis set dependence. Similar empirical approaches have been suggested and used in previous work.[37,58,71,72] The procedure (superposition correction and dipole scaling) does not affect the overall shape of the potential energy surface and the location of energy minima because the geometry is determined primarily by strong short-range forces. However, it has a large effect on the interaction energy. The consistent convergence of the scaled results for different basis sets and the good agreement with experimental data suggest that the empirical correction procedure is able to correct for the systematic biases of the *ab initio* calculations.

An important element of the present potential is that it includes ion-induced polarization of the peptide group. This is essential to reproduce correctly the intermediate range (3 to 5 Å) distance dependence ($1/r^4$) of the potential function. Such polarization effects are represented by atomic polarizability coefficients. All the parameters were adjusted to reproduce the *ab initio* calculations modified by the empirical correction procedure of eq. (1). The adjustments of the parameters to reproduce the *ab initio* calculations were done manually because automatic fitting procedures did not produce satisfactory results. The parameters given in Table VI represent a first step in the development of an accurate ion–peptide potential function. The parameters of the potential function (i.e., the polarizability coefficients, the van der Waals, and the core size), are adjusted to reproduce the salient features of the *ab initio* potential surface. It is expected that refinements of this parameterization may be necessary to reproduce experimental free energies in dense systems, such as the binding of Na^+ to the gramicidin channel.[63,73]

In the case acetamide and NMA, the potential function was constructed as a superposition of pairwise additive terms varying as $1/r^4$ with no intramolecular electrostatic interactions between the induced dipoles. This approximation accounts only the first-order polarization (i.e., the induced polarization is not determined self-consistently and the dipoles induced by the ion are not influenced by other partial charges or by other induced dipoles[74–76]). In large systems, this results in a pairwise additive potential function, and higher order

nonpairwise additive effects are neglected. To account for many-body effects, second-order partial charge induced-dipole and third-order induced-dipole/induced-dipole interactions must be included.[63] The first-order approximation has been used in initial studies of ion transport in the gramicidin channel,[8-10] and the second-order approximation has been used in thermodynamic study of double ion occupancy in the gramicidin channel.[73] The importance of nonadditivity in ion–peptide interactions has been investigated by studying the binding of Na^+ to the gramicidin channel using molecular dynamics simulations and *ab initio* calculations.[63] Further tests of the potential function can be made by calculations of crystal structures of metal ions with NMA[77] and by simulations of bulk solutions of amides.[78,79] In future work, the ion–peptide potential energy function will be extended to describe the interaction of ions with protein sidechains as part of a project to develop a protein potential function including all atoms.[80]

Acknowledgments

We are grateful to Jiali Gao for providing the frequencies for the zero point corrections, to Eric Wimmer and John Mertz of CRAY Research for their assistance, and to CRAY Research for providing the CRAY X-MP time used for all the *ab initio* calculations. The work reported here was supported in part by a grant from the National Science Foundation.

Appendix A: Basis Sets for K^+

For the convenience of the reader, we give in this appendix the 3-21G basis set coefficients of Hehre[41-43] and Sakai[44] and the 6-31G basis set coefficients of Wachters[47] with the contraction of Clementi[48] for K^+ ions as they appear in an input file for GAUSSIAN 86.[40]

K^+ 3-21G BASIS SET

Potassium ion 3-21G SCF = −596.006597 Hartree

```
1 1
K
K 0
S 3 1.0
          1719.59267000     0.0649400
           259.84607000     0.3810100
            56.61061000     0.6771500
SP 3 1.00
            71.55720000    -0.1093429     0.1339654000
            15.43894000     0.1130640     0.5302673000
             4.47455100     0.9462575     0.5117992000
SP 3 1.00
             4.12127500    -0.2699730     0.0199492200
             1.18862100     0.3646323     0.4340213000
             0.37567380     0.8107533     0.6453226000
SP 2 1.00
             0.24457660    -0.2688250     0.0003081035
             0.03897175     1.1289830     0.9998787000
SP 1 1.00
             0.01606255     1.00          1.00
* * *
```

K^+ 6-31G BASIS SET

#HF/GEN
Potassium ion 6-31G SCF = −598.965954 Hartree

```
1 1
K
K 0
S 6 1.00
          150591.000000     0.000595
           22629.600000     0.004541
            5223.160000     0.023246
            1498.065000     0.091652
             495.165000     0.292354
             180.792000     0.675344
S 2 1.00
              71.194000     0.658838
              29.372300     0.373290
S 2 1.00
               8.688630    -0.461451
               3.463820    -0.575610
S 2 1.00
               0.811307     0.486595
               0.312555     0.553452
S 1 1.00
               0.035668     1.000000
S 1 1.00
               0.016517     1.000000
P 6 1.00
             867.259000     0.002419
             205.254000     0.019431
              65.821400     0.089547
              24.574200     0.258787
               9.877040     0.444183
               4.116930     0.363814
P 1 1.00
               1.556530     1.000000
P 2 1.00
               0.614068     0.672231
               0.228735     0.392736
* * *
```

Appendix B: Zero Point Energy

As an example, we consider the corrections to the affinities of Li^+ with water necessary to compare with the experimental enthalpies of binding.[17] The binding constant $K(T)$ was defined experimentally at constant pressure as[17]

$$K(T) = \frac{[H_2O—Li]}{P_{H_2O}[Li]} \tag{A.1}$$

where P_{H_2O} is the partial pressure of water equal to $[H_2O]k_BT$. The binding enthalpy was extracted with the vant Hoff relation by plotting $-k_BT$ ln $K(T)$ as a function of $1/T$. From statistical mechanics[62] the concentration ratio is

$$\frac{[H_2O—Li]}{[H_2O][Li]} = \frac{(q_{trans}^{H_2O—Li}/V)}{(q_{trans}^{H_2O}/V)(q_{trans}^{Li}/V)} \times \frac{q_{rot}^{H_2O—Li}}{q_{rot}^{H_2O}} \frac{q_{vib}^{H_2O—Li}}{q_{vib}^{H_2O}} \tag{A.2}$$

where the various terms are, respectively, the translational (q_{trans}), rotational (q_{rot}), and vibrational (q_{vib}) partition functions of the species. The effects of electronic excited states have been neglected. Evaluating the partial derivative of the binding constant, eq. (A.1), with respect to the temperature gives

$$\frac{\partial \ln K(T)}{\partial(-1/k_BT)} = \Delta E_{pot} + \Delta E_{trans} + \Delta E_{rot} + \Delta E_{PV} + \Delta E_{zpe} + \Delta E_{vib} \tag{A.3}$$

where ΔE_{pot} is the difference in potential energy, $E_{H_2O—Li} - E_{H_2O} - E_{Li}$), and the various terms are

$$\Delta E_{trans} = -1.5\, k_BT$$

$$\Delta E_{rot} = 0.0\, k_BT$$

$$\Delta E_{PV} = -1.0\, k_BT$$

$$\Delta E_{zpe} = 0.5\left[\sum_{i=1}^{6} h\nu_i^{H_2O—Li} - \sum_{i=1}^{3} h\nu_i^{H_2O}\right]$$

$$\Delta E_{vib} = \left[\sum_{i=1}^{6} f(h\nu_i^{H_2O—Li}) - \sum_{i=1}^{3} f(h\nu_i^{H_2O})\right] \tag{A.4}$$

where the function $f(x) = x/(\exp(x) - 1)$ in E_{vib}. The normal frequencies, calculated at the HF/6-31G** level, are 1769.4523, 4148.3877, and 4265.4223 cm^{-1} for the isolated water molecule, and 439.6280, 562.3707, 582.9308, 1795.6094, 4087.3193, and 4173.3519 cm^{-1} for the water–Li^+ complex. The enthalpies were extracted experimentally at temperatures around 600 K. At this temperature, the zero point energy E_{zpe} is 1.73 k_BT and the vibrational energy E_{vib} is 1.49 k_BT, leading to a total correction to the interaction energy

$$\left|\frac{\partial \ln K(T)}{\partial(-1/k_BT)}\right|_{T=600\text{ K}} = \Delta E_{pot} + (-1.5 - 1.0 + 1.74 + 1.34)k_BT \tag{A.5}$$

The total correction is less than 0.75 kcal/mol (i.e., within the accuracy of the present calculations). Similar corrections are found for Na^+ and K^+.

References

1. D. H. Mackay, P. H. Berens, and K. R. Wilson, *Biophys. J.*, **46**, 229 (1983).
2. K. S. Kim and E. Clementi, *J. Am. Chem. Soc.*, **107**, 5504 (1985).
3. C. Etchebest and A. Pullman, *J. Biomol. Struc. Dyn.*, **3**, 805 (1986).
4. A. Pullman, *Quat. Rev. Biophys*, **20**, 173 (1987).
5. P. C. Jordan, *J. Phys. Chem.*, **91**, 6582 (1987).
6. P. C. Jordan, *Transport through Membranes: Carriers, Channels and Pumps*, Kluwer Academic, Boston, 1988, p. 237.
7. S. W. Chiu, J. A Novotny, E. Jakobsson, and J. A. McCammon, *Biophys. J.*, **64**, 98 (1993).
8. B. Roux and M. Karplus, *Biophys. J.*, **59**, 961 (1991).
9. B. Roux and M. Karplus, *J. Phys. Chem.*, **95**, 4856 (1991).
10. B. Roux and M. Karplus, *J. Am. Chem. Soc.*, **115**, 3250 (1993).
11. B. Roux and M. Karplus, *Ann. Rev. Biomol. Struc. Dyn.*, **23**, 731 (1994).
12. O. S. Andersen, *Ann. Rev. Physiol.*, **46**, 531 (1984).
13. A. S. Arseniev, V. F. Bystrov, T. V. Ivanov, and Y. A. Ovchinnikov, *FEBS Lett.*, **186**, 168 (1985).
14. H. L. Friedman and C. V. Krishnan, *Water: A Comprehensive Treatise*, Vol. 3, Plenum Press, New York, 1973.
15. B. Hille, *Ionic Channels of Excitable Membranes*, Sinauer, Sunderland, MA, 1984.
16. C. L. Brooks III, Martin Karplus, and B. M. Pettitt, *Proteins. A Theoretical Perspective of Dynamics, Structure and Thermodynamics*, John Wiley & Sons, New York, 1988.

17. I. Džidić and P. Kebarle, *J. Phys. Chem.*, **74**, 1466 (1970).
18. P. Kebarle, *Ann. Rev. Phys. Chem.*, **28**, 445 (1977).
19. W. R. Davidson and P. Kebarle, *J. Am. Chem. Soc.*, **98**, 6133 (1976).
20. P. Kebarle, G. Caldwell, T. Magnera, and J. Sunner, *Pure & Appl. Chem.*, **57**, 339 (1985).
21. R. H. Stanley and J. L. Beauchamp, *J. Am. Chem. Soc.*, **97**, 5920 (1975).
22. R. L. Woodin and J. L. Beauchamp, *J. Am. Chem. Soc.*, **100**, 501 (1978).
23. A. Pullman and P. Schuster, *Chem. Phys. Lett.*, **24**, 472 (1974).
24. V. Renugopalakrishnan and D. W. Urry, *Biophys. J.*, **24**, 729 (1978).
25. J. F. Hinton, A. Beeler, D. Harpool, D. W. Briggs, and A. Pullman, *Chem. Phys. Lett.*, **47**, 411 (1977).
26. P. A. Kollman, *Chem. Phys. Lett.*, **55**, 555 (1978).
27. P. G. Mezey, G. Del Re, P. Otto, and J. Ladik, *Int. J. Quant. Chem.*, **21**, 677 (1982).
28. D. N. Fuchs and B. M. Rode, *Chem. Phys. Lett.*, **82**, 517 (1981).
29. C. Nagata and M. Aida, *J. Theor. Biol.*, **110**, 569 (1984).
30. N. Gresh, A. Pullman, and P. Claverie, *Int. J. Quant. Chem.*, **28**, 757 (1985).
31. G. Conrongiu, E. Clementi, E. Pretsch, and W. Simon, *J. Chem. Phys.*, **70**, 1266 (1979).
32. G. Conrongiu, E. Clementi, E. Pretsch, and W. Simon, *J. Chem. Phys.*, **72**, 3096 (1980).
33. A. T. Hagler, E. Huler, and S. Lifson, *J. Am. Chem. Soc.*, **96**, 5319 (1976).
34. U. Burkert and N. L. Allinger, *Molecular Mechanics*, American Chemical Society, Washington, DC, 1982.
35. F. A. Momany, R. F. McGuire, A. W. Burgess, and H. A. Scheraga, *J. Am. Chem. Soc.*, **79**, 2361 (1975).
36. W. L. Jorgensen and J. Tirado-Rives, *J. Am. Chem. Soc.*, **110**, 1657 (1988).
37. S. J. Weiner, P. A. Kollman, D. A. Case, U. C. Singh, C. Ghio, G. Alagona, S. Profeta, Jr., and P. Weiner, *J. Am. Chem. Soc.*, **106**, 765 (1984).
38. B. R. Brooks, R. E. Bruccoleri, B. D. Olafson, D. J. States, S. Swaminathan, and M. Karplus, *J. Comp. Chem.*, **4**, 187 (1983).
39. Gaussian 82. J. S. Binkley, M. Frisch, R. Krishnan, D. J. DeFrees, H. B. Schlegel, R. A. Whiteside, E. Fluder, R. Seeger, and J. A. Pople, Carnegie Melon University, Quantum Chemistry Publishing Unit, Pittsburgh, PA, 1982.
40. Gaussian 86. M. J. Frisch, J. S. Binkley, H. B. Schlegel, K. Raghavachari, C. F. Melius, R. L. Martin, J. J. P. Steward, F. W. Bobrowicz, C. M. Rohlfing, L. R. Kahn, D. J. Defrees, R. Seeger, R. A. Whiteside, D. J. Fox, E. M. Fleuder, and J. A. Pople, Carnegie Melon University, Quantum Chemistry Publishing Unit, Pittsburgh, PA, 1986.
41. K. D. Dobbs and W. J. Hehre, *J. Comp. Chem.*, **7**, 359 (1986).
42. J. S. Binkley, J. A. Pople, and W. J. Hehre, *J. Chem. Phys.*, **102**, 939 (1980).
43. W. J. Pietro, M. M. Franci, W. J. Hehre, D. J. DeFrees, J. A. Pople, and J. S. Binkley, *J. Am. Chem. Soc.*, **104**, 5039 (1982).
44. Y. Sakai, H. Tatewaki, and S. Huzinaga, *J. Comp. Chem.*, **2**, 100 (1981).
45. W. J. Hehre, R. Ditchfield, and J. A. Pople, *J. Chem. Phys.*, **56**, 2257 (1972).
46. P. C. Hariharan and J. A. Pople, *Theoret. Chim. Acta*, **23**, 213 (1973).
47. A. J. H. Wachters, *J. Chem. Phys.*, **52**, 1033 (1970).
48. L. Gianolio, R. Pavani, and E. Clementi, *Gaz. Chim. It.*, **108**, 181 (1978).
49. S. F. Smith, J. Chandrasekar, and W. L. Jorgensen, *J. Am. Chem. Soc.*, **86**, 3308 (1982).
50. R. L. Cook, *J. Mol. Spect.*, **53**, 62 (1974).
51. M. Kitano and K. Kuchitsu, *Bull. Chem. Soc. Jap.*, **46**, 3048 (1973).
52. M. Kitano, T. Fukuyama, and K. Kuchitsu, *Bull. Chem. Soc. Jap.*, **46**, 384 (1973).
53. V. S. Dimitrov and J. A. Ladd, *J. Mol. Struct.*, **159**, 107 (1987).
54. After completion of the calculations, the structure of DMF determined by gas phase electron diffraction appeared in press; see G. Schultz and I. Hargittai, *J. Phys. Chem.*, **97**, 4966 (1993).
55. S. F. Boys and F. Bernardi, *Mol. Phys.*, **19**, 553 (1970).
56. H. Berthod and B. A. Pullman, *Chem. Phys. Lett.*, **70**, 434 (1980).
57. W. J. Hehre, L. Radom, P. R. Schleyer, and J. A. Pople, *Ab Initio Molecular Orbital Theory*, John Wiley & Sons, New York, 1986.
58. W. E. Reiher III, *Theoretical Studies of Hydrogen Bonding*, Ph.D. thesis, Harvard University, Cambridge, MA, 1985.
59. A. C. Hopkinson, *Applications of MO Theory in Organic Chemistry*, vol. 2, Elsevier, New York, 1977, p. 194.
60. T. R. Dyke and J. S. Muenter, *J. Chem. Phys.*, **59**, 3125 (1973).
61. R. M. Meighan and R. H. Cole, *J. Phys. Chem.*, **68**, 503 (1964).
62. D. A. McQuarrie, *Statistical Mechanics*, Harper & Row, New York, 1976.
63. B. Roux, *Chem. Phys. Lett.*, **212**, 231 (1993).
64. P. A. Kollman and I. D. Kuntz, *J. Am. Chem. Soc.*, **94**, 9236 (1972.
65. T. P. Lybrand and P. A. Kollman, *J. Phys. Chem.*, **83**, 2923 (1985).
66. J. Åqvist, *J. Phys. Chem.*, **94**, 8021 (1990).
67. D. R. Lide, Ed., *CRC Handbook of Chemistry and Physics*, 72nd ed., CRC Press Inc., Boca Raton, FL, 1992.
68. L. Pauling, *Nature of the Chemical Bond and Structure of Molecules and Crystals*, 3rd ed., Cornell University Press, Ithaca, NY, 1960.
69. S. Lifson, A. R. Hagler, and P. Dauber, *J. Am. Chem. Soc.*, **101**, 5111 (1979).
70. A. T. Brünger, M. Karplus, and G. A. Petsko, *Acta Cryst.*, **A45**, 50 (1989).
71. U. C. Singh and P. A. Kollman, *J. Comp. Chem.*, **5**, 129 (1984).
72. S. R. Cox and D. E. Williams, *J. Comp. Chem.*, **2**, 304 (1981).

73. B. Roux, B. Prod'hom, and M. Karplus, *Biophys. J.* (1995) to be published.
74. D. V. Belle, I. Couplet, M. Prevost, and S. J. Wodak, *J. Mol. Biol.*, **198**, 721 (1987).
75. J. M. Goodfellow, J. L. Finney, and P. Barnes, *Proc. R. Soc. Lond.*, **214**, 213 (1982).
76. B. J. Gellatly, J. E. Quinn, P. Barnes, and J. L. Finney, *Mol. Phys.*, **59**, 949 (1983).
77. P. Chakrabarti, K. Venkatesan, and C. N. R. Rao, *Proc. R. Soc. Lond. A*, **375**, 127 (1981).
78. J. S. Falcone and R. H. Wood, *J. Sol. Chem.*, **3**, 215 (1974).
79. B. G. Cox, G. R. Hedwig, A. J. Parker, and D. W. Watts, *Aust. J. Chem.*, **27**, 477 (1974).
80. A. D. Mackerell, Jr., D. Bashford, M. Bellot, R. L. Dunbrack, M. J. Field, S. Fischer, J. Gao, H. Guo, D. Joseph, S. Ha, L. Kuchnir, K. Kuczera, F. T. K. Lau, C. Mattos, S. Michnick, D. T. Nguyen, T. Ngo, B. Prod'hom, B. Roux, M. Schlenkrich, J. Smith, R. Stote, J. Straub, J. Wiorkiewicz-Kuczera, and M. Karplus, *Biophys. J.*, **61**, A143 (1992).